Hindawi
International Journal of Photoenergy
Volume 2023, Article ID 2454612, 15 pages
https://doi.org/10.1155/2023/2454612

Research Article

Experimental Study on the Effect of In/Out Radial-Finned Heat Sink with PCM under Constant and Intermittent Power Mode in Power LEDs

Thangamani Ramesh,[1,2] **Ayyappan Susila Praveen**,[1] **Praveen Bhaskaran Pillai**,[3] **Sachin Salunkhe**,[4] **Adham E. Ragab**,[5] **Hussein M. A. Hussein**,[6,7] **and Paulo Davim**[8]

[1]*Department of Mechanical Engineering, Vel Tech Rangarajan Dr. Sagunthala R&D Institute of Science and Technology, Chennai 600062, Tamil Nadu, India*
[2]*Department of Mechanical Engineering, Kalasalingam Academy of Research and Education, Krishnankoil 626126, Tamil Nadu, India*
[3]*Clean Energy Research Group, Department of Mechanical and Aeronautical Engineering, University of Pretoria, Pretoria 0002, South Africa*
[4]*Department of Biosciences, Saveetha School of Engineering, Saveetha Institute of Medical and Technical Sciences, Chennai, India*
[5]*Department of Industrial Engineering, College of Engineering, King Saud University, Riyadh, Saudi Arabia 11421*
[6]*Mechanical Engineering Department, Faculty of Engineering and Technology, Future University in Egypt, New Cairo 11835, Egypt*
[7]*Mechanical Engineering Department, Faculty of Engineering, Helwan University, Cairo 11732, Egypt*
[8]*University of Aveiro, Department of Mechanical Engineering, Campus Universitário de Santiago, 3810-193 Aveiro, Portugal*

Correspondence should be addressed to Thangamani Ramesh; ramesh.ramesh81@gmail.com

Received 7 October 2022; Revised 6 February 2023; Accepted 25 November 2023; Published 22 December 2023

Academic Editor: Chaofan Sun

The findings of the experimental study into optimizing the heat transfer rate of a PCM-based heat sink for high-power LEDs are presented in this work. The study investigated five heat sink types, with and without PCM. The LED case and junction temperatures, LED module temperatures, heat storage and release rate analyses, analyses of three types of cyclic operation modes, luminous flux, and heat sink thermal resistance were all examined independently. The results indicated that the PCM-based LED heat sink had improved thermal performance. The LED junction temperature of the PCM-equipped E-20 heat sink is nine degrees Celsius lower at 10 W than that of the heat sink without PCM. Furthermore, the E-20 heat sink with PCM extends the LED module's critical lifespan. As a bonus, the E-20 with PCM had a 38.19 percent lower thermal resistance at 10 W than the E-20 without PCM. According to these results, the heat sink E-20 emits 715 lm at 10 W when operated without a phase-change material (PCM). With the same input power, the luminous flux of an E-20 equipped with a heat sink and a phase-change material (PCM) is 750 lm, a gain of 4.7%. Finally, clearly recommend the heat E-20 sink with PCM suitable for high-power LED thermal management system.

1. Introduction

In recent years, light-emitting diode (LED) has been used in various applications like downlights, headlamps in automobiles, indoor/outdoor, and stage lighting. LED has more advantages such as extended service time, low power cost, high energy efficiency, high reliability, and eco-friendly than traditional lighting systems [1]. However, when LEDs operate at 80% of the electric energy, it gets converted to waste heat energy. While the remaining 20% of the electric energy only gets converted to visible light [2]. The LED junction temperature rapidly increases due to insufficient heat dissipated, decreasing the light LED's life [3]. Hence, effective thermal management techniques are required to high-power LED lighting systems for proper heat dissipation [4]. There are two possible thermal management options:

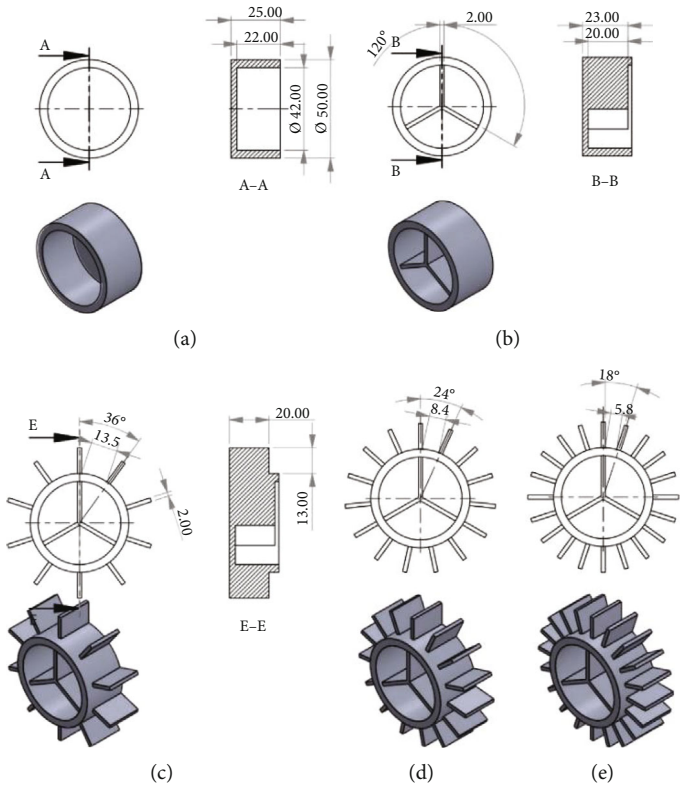

Figure 1: Isometric views of heat sinks with different configurations: (a) E0I0, (b) E0I3, (c) E10I3, (d) E15I3, and (e) E20I3.

active and cooling systems. Active cooling typically requires an external force for proper heat transfer, whereas passive cooling dissipates waste heat to the ambient through free convection and radiation heat transfer [5]. Therefore, many researchers developed LED heat sinks using the passive cooling method [6, 7] to improve the cooling performance of LEDs.

Park et al. [8] conducted a multidisciplinary design optimization and experimental investigation of cooling efficiency in the chimney-based radial heat exchangers. The results of this experimental work disclosed that the heat rejection efficiency of a chimney-based radial heat sink increases up to 20% due to cooling airflow to the heat sink center. Sundar et al. [9] studied the performance of a heat exchanger having a circular base radial short-finned heat exchanger that had perforations under convection mode heat transfer, experimentally. They compared their results with the finned heat exchangers that did not have any perforations. They observed that the perforated heat sink shows significant thermal performance. Yu et al. [10] investigated the influence of heat sink geometry on the heat dissipation performance of circular-based and rectangular fins under natural convection. The results indicated that when the number of fins is fewer than 36, the thermal resistance of the heat sink is reduced. Haghighi et al. [11] presented a plate cubic pin fin heat sink for a 120 W electronic application. They concluded that the heat transfer enhancement of plate cubic pin fin heat sink is up to 41.6%, compared with a standard plate fins heat sink. Feng et al. [12] developed a novel cross-fin heat sink to improve heat dissipation in high-powered LED applications. The convective and total heat transfer coefficients of the cross-finned heat exchanger rose by 11% and 15%, respectively, as compared to the plate-fin heat sink. Recently, relatively few research (both experimental and numerical) on PCM-based heat sinks for high-power LED applications have been undertaken [13–17]. The PCM consists of three general thermal storage modes: sensible heat, latent heat, and thermochemical energy. Within these models, latent heat storage after PCM has received significant consideration. This is because it provides a better energy storage ability and a slight change in temperature throughout the phase transition process. The disadvantage of the thermal conductivity of PCM is very low. This problem can be overcome by using high thermal conductivity materials with different geometry fins in combination with PCM and increasing the heat transfer rate [18–25]. Ashraf et al. [26] investigated the effect of pin-fin geometric (circular pin, square pin) heat sink experimentally to compare its performance with six different paraffin (paraffin, RT-54, RT-44, RT-35HC, SP-31, and n-eicosane). It was concluded from these results that 8 W input power paraffin wax was the best PCM with the highest enhancement ratio. El-Said et al. [27] studied the air injection flow rate analysis using machine-learning algorithms.

Hosseinizadeh et al. [28] studied the performance of heat exchangers having PCM in their heat sink while varying their fin thickness such as 2 mm, 4 mm, and 6 mm. The 4 mm fin thinness exhibited better heat transfer performance, followed by 2 mm and 6 mm. A new composite material- (copper-powder-sintered frame/paraffin) based heat sink was prepared by Li et al. [29] for high thermal conductivity and temperature cycling stability without leakage. It reveals that the LED brightness with the new composite material-based heat sink increased by 4.07% compared to

Table 1: Design parameters for each heat sink used in this experimental work.

Heat sink type	Number of fins	Overall height of heat sink (mm)	Fin height (mm)	Fin length (mm)	Fin thickness (mm)	The outer radius of the heat sink (mm)	The inner radius of the heat sink (mm)	The thickness of the base (mm)	Heat sink surface area (mm^2)
E0I0	—	25	—	—	—	50	44	3	10756.81
E0I3	3		20	21	2				13084.63
E10I3	10								18812.79
E15I3	15			13					21676.87
E20I3	20								24540.95

the heat sink made of aluminum. Yagci et al. [30] experimentally investigated the melting as well as solidification characteristics of PCM in a vertical tube and shell unit with three different fin edge length ratios ($w1/w2 = 1, 1/3$, and 0). They observed that the PCM total melting time of edge length ratios 1/3 and 0 was lowered by 58% and 62%, respectively, when compared to edge length ratio 1. Arshad et al. [31] experimentally reported the effects of pin thickness which was 1 mm, to 3 mm in steps of 1 mm and volume fraction of 0.00, 0.33, 0.66, and 1.00, respectively, of PCM for electronic cooling applications. The results reveal that a 2 mm thick pin-finned heat exchanger filled with a PCM achieves optimum thermal efficiency in operation time (volumetric ratio of 1.00). The microencapsulated paraffin with low metal alloy material preparation was experimentally investigated by Praveen and Suresh [32] for applications of passive heat sinks and stated that the heat sink with fins and microencapsulated PCM/low metal alloy cooling rate increased compared to finned without PCM. Praveen et al. [33] observed the performance of the heat exchanger that contained graphene nanoplatelets. For the paraffin-filled heat sink, the nanoplatelets were encapsulated with 0.5, 1, and 3 wt% composite PCM. They determined that introducing graphene nanoplatelets packed with encapsulated PCM delays the rate at which the heat sink's temperature rises by 22.5% at 10 W input power. Various composite PCM materials were developed recently for application in thermal energy storage for PCM-based heat sinks, including glycol/CuO [34], macropacked neopentylglycol with CuO nanoparticles [35], and pentaerythritol with alumina (Alo_3) particles [36]. According to the study, a paraffin-filled heat sink-based heat sink is suited for good thermal control.

In the present study, various aspects of a heat sink filled with PCM coupled to LED are experimentally investigated for efficient thermal management. The main objective is to explore different configurations of heat sinks with PCM to reduce the LED case and junction temperatures under natural conditions for LED downlight applications. For this purpose, five different configuration heat sinks with and without PCM are considered under three input power. This experimental work is on performing a PCM characterization study to find thermophysical properties, determine LED case and junction temperature variations and define PCM-based heat sink thermal performance, evaluate the LED module temperature distribution of the heat sinks with and without PCM, study the heat storage and release rate of the different configuration heat sink with and also without PCM, investigate the three modules using intermittent input power, study the LED luminous flux, compare the heat sink thermal resistance of heat sink with and without PCM, and study the enhancement ratio for various configurations of the heat sinks.

2. Experimental Work

2.1. Design and Fabrication of Heat Sink. In this work's design and construction of the five configurations of PCM-based aluminum alloy (6063), heat sinks are shown in Figure 1. All the heat sinks were fabricated by the process of vertical milling, namely, the no external and internal fin heat sink (called E0I0), no external and three internal radial-finned heat sink (E0I3), ten external and three internal radial-finned heat sink (E10I3), fifteen external and three internal radial-finned heat sink (E15I3), and twenty external and three internal radial-finned heat sinks (E20I3). The fabricated heat sink-detailed design parameters are given in Table 1. In this experimental study, the volume fractions of the fins in the heat sinks connected to the LED bulbs are calculated using

$$\varphi = \frac{V_{\text{fin}}}{V_{\text{total}} - V_{\text{fin}}}, \tag{1}$$

where φ, V_{fin}, and V_{total}, respectively, are the fin volume fraction of the fin, the volume of the individual fin (mm^3), and the volume of the heat sink (mm^3). The prior findings [37, 38] demonstrate that optimal thermal efficiency is reached when a proportion of a heat sink's fin volume is about 9%.

Table 2: Specification of the white LED module.

LED parameter	Value	Unit
Driving current	360-900	mA
Voltage	40	V
Maximum junction temperature	125	°C
Size (length × width)	19 × 19	mm

2.2. LED and Power Supply. For this research, a commercial LED (LUSTRON LL610F-Cool white) module was selected for downloading light application; its specification is shown in Table 2. The size of the LED module is 19 × 19 mm. The LED module considers the maximum permissible junction temperature to be 125°C (datasheet by manufacturer). To decrease the thermal resistance at the contact surface and air gap, thermal grease (HALINZIYE Shenzhen-HY 510) as a thermal interface material is necessary to apply between the surfaces of the LED module and heat sinks. The high-power LED is fixed below the heat sink with the help of an M3 screw. An adjustable DC power supply (60 V/3A, KUSAM-MECO-KM-PS-302D-II) to provide input power was connected to LED module; positive and negative terminals are shown in Figure 2.

2.3. Data Reduction. The dissipative power (P_d) in Watts can be calculated using equation (2). The P_d means high-power LEDs, 20% of the total electrical energy only is converted to visible light, and the remaining 80% of waste heat energy is dissipated from the junction.

$$P_d = P_e - P_u, \tag{2}$$

where P_e and P_u are the energy supplied to LED (W) and energy utilized (W), respectively.

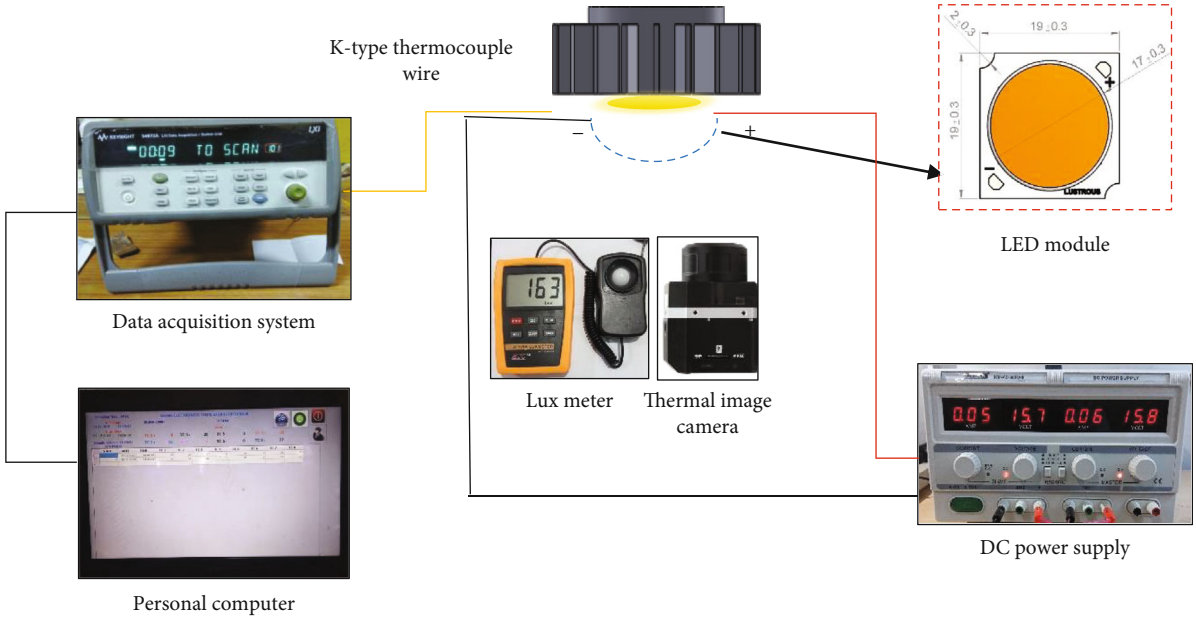

Figure 2: Schematic of the experimental setup.

The junction temperature (T_j) is related to the case temperature (T_c). Each experiment was repeated thrice, and the junction temperatures were determined using

$$T_j = T_c + P_d \times R_{j-c}, \tag{3}$$

where R_{j-c} is the junction to the case thermal resistance, and its value is 1.9 W/°C (available in the LED module manufacturer datasheet). The T_c is case temperature values collected using a K-type thermocouple with the interval of one min. The K-type thermocouple was coupled to the personal computer- (PC-) based temperature data logging system (KEYSIGHT Technologies, 34972A).

To estimate the temperature fluctuation of the LED module using an infrared thermal image camera (FLIR, FLIR Vue Pro R 640) with an accuracy of 5%, the heat sink thermal resistance has been calculated by

$$R_h = \frac{T_b - T_a}{P_d}, \tag{4}$$

where T_b and T_a are the temperatures of interface material (°C) and ambient temperature, respectively.

2.4. PCM Material. In this experimental work, lauric acid was used as the PCM supplied by Sigma-Aldrich-W261416. To measure PCM's latent heat capacity and phase change temperature by using differential scanning calorimetry (DSC, Q200, Waters Austria) at CSIR Chennai, the DSC heating and cooling rate of 5°C/min and operating temperatures ranging from 30 to 100°C are followed.

2.5. Experimental Uncertainty Analysis. The uncertainty of fundamental parameters such as voltage and current was measured by calibrating the corresponding measuring devices. The measured quantities are shown in Table 3 as the tolerance limit or most minor count obtained from the respective measuring devices. For example, during the calibration of the thermocouples, the readings were accurate within a tolerance of ±0.5°C. However, the uncertainty for the derived parameters, i.e., the power required, was calculated as shown in equation (5). The result obtained is shown in Table 3.

Table 3: Uncertainty results.

Sl. no	Quantity measured	Uncertainty
1	Temperature (°C)	±0.5
2	Voltage (V)	±0.337
3	Current (A)	±0.008
4	Power (%)	±2.864

$$\begin{aligned}
\sigma_p &= \pm\sqrt{\left(\frac{\partial P}{\partial V}\sigma_V\right)^2 + \left(\frac{\partial P}{\partial I}\sigma_I\right)^2},\\
\sigma_p &= \pm\sqrt{(0.30 \times 0.337)^2 + (33.5 \times 0.008)^2},\\
\sigma_p &= 0.286,\\
\frac{\sigma_p}{P} &= 0.028,\\
\sigma_p &= 2.86\%.
\end{aligned} \tag{5}$$

3. Results and Discussion

3.1. PCM Characterization. The PCM melting temperature and latent heat values are plotted in Figure 3. The results revealed that the PCM latent heat and peak melting temperature values are 217 J/g and 45°C by DSC analysis, as the DSC results show the thermophysical properties of PCM appropriate for the storage of latent heat energy for heat sink applications.

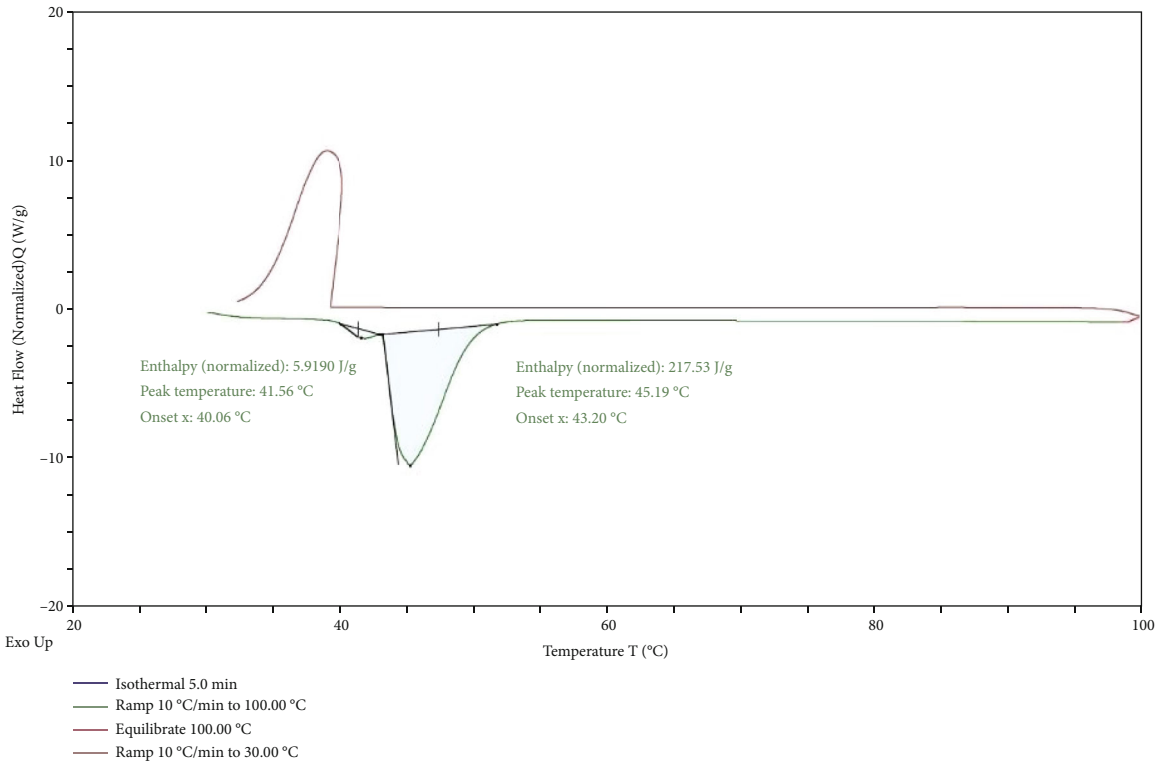

Figure 3: DSC curve of PCM.

3.2. LED Case Temperature Effect on Heat Sink Different Configuration (without PCM). This experimental work applies three different input powers (electrical) of 4 W, 10 W, and 16 W to the LED module under natural convection. The LED case temperature is used to predict the heat transfer performance of the LED. The LED case temperature values of the heat sink with different configurations (E0I0, E0I3, E10I3, E15I3, and E20I3) without PCM are shown in Figures 4(a)–4(c). It can be observed that the LED case temperature increased gradually concerning the time at all input power, comparatively without extended radial fins (E0I0 and E0I3). When extended radial fins (E0I0, E0I3, E10I3, E15I3, and E20I3) were used, the LED case temperature decreased overall up to 50.35%. This decrease in case temperature is because of the rise in the contact surface area of the heat sinks associated with ambient temperature. In turn, it creates a natural convective current, thereby heats removed from the system. This justifies that the heat transfer capability of the heat sinks E10I3, E15I3, and E20I3 is superior to that of the heat sinks E0I0 and E0I3. Figure 4(a) shows that the case temperature measured after 90 min is 53°C, 51°C, 44°C, 43°C, and 41°C for E0I0, E0I3, E10I3, E15I3, and E20I3, respectively, at 4 W input power. The next level experiment of increasing the input power from 4 W to 10 W is related to the case temperature distribution shown in Figure 4(b). It was found that the LED T_c for the heat sink E20I3 decreased by approximately 27.83% when correlated with the heat sink at 10 W input power coded as E0I3 and devoid of the PCM.

3.3. LED Case Temperature Effect on Heat Sink Different Configuration (with PCM). In this section, the heat transfer performance under varying times for different configurations of heat sinks (E0I0, E0I3, E10I3, E15I3, and E20I3) with PCM was studied based on the LED case temperature variation recorded by K-type thermocouple solder at the negative terminal of the LED module with input power levels of 4 W, 10 W, 16 W. Figures 5(a)–5(c) present the case temperature values for PCM-filled heat sinks. The figures show that the case temperature is increasing and gradually slowing down compared to without PCM-based LED heat sinks. This indicates that the PCM is absorbing more heat, using the high latent heat capacity of the PCM.

Figures 4(b) and 5(b) show the PCM-filled heat sink E20I3 and LED T_c reduced by 16.36% than that of the heat sink E20I3 without PCM at 10 W. This effect is due to the combined effect of increased heat absorption rate by PCM and increased convection rate by the fins outside. The heat sink E20I3 configuration radial fins have more surface area in contact with cooling air, which creates the required heat transfer. The natural convection, current, and high latent heat PCM filled the inside of the heat sink. These results suggest that a PCM-based E20I3 heat sink can be used as an effective passive heat sink in thermal management for LED downlight applications.

3.4. Junction Temperature Effect on Heat Sink Different Configuration (without PCM). The LED junction temperature concerning the time at three different input powers is depicted in Figures 6(a)–6(c). It is shown that the T_j for heat sinks E10I3, E15I3, and E20I3 without PCM are less than the heat sinks E0I0 and E0I3 at 4 W, 10 W, and 16 W input power. Figure 6(a) shows that the junction temperatures noted after 90 min are 59°C, 57°C, 50°C, 49°C, and 47°C for

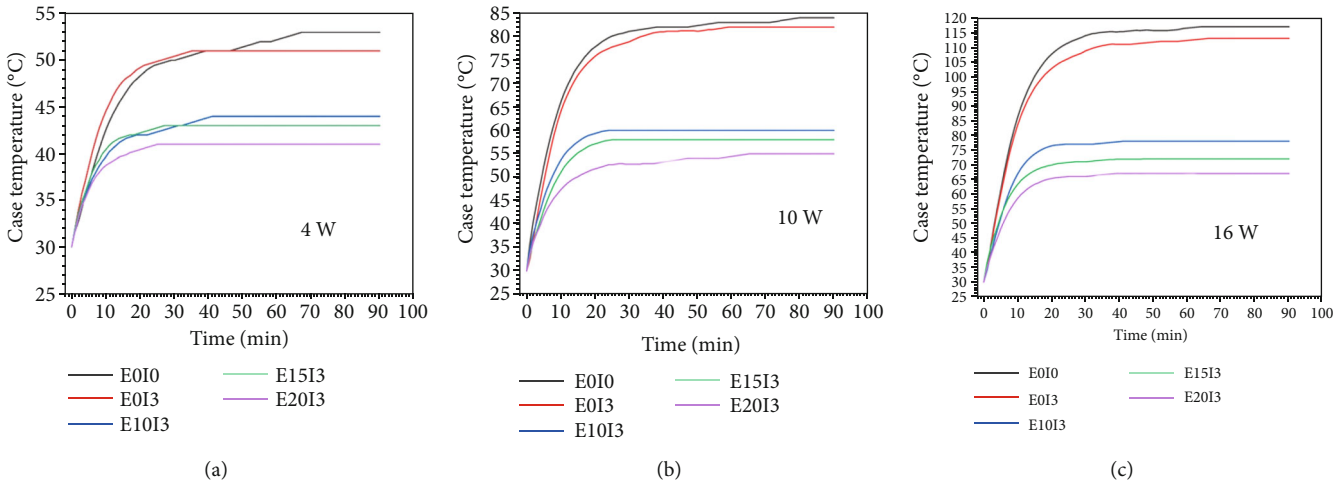

Figure 4: LED case temperatures versus time that are taken by the various configurations of the heat sink without PCM at various input powers: (a) 4 W, (b) 10 W, and (c) 16 W.

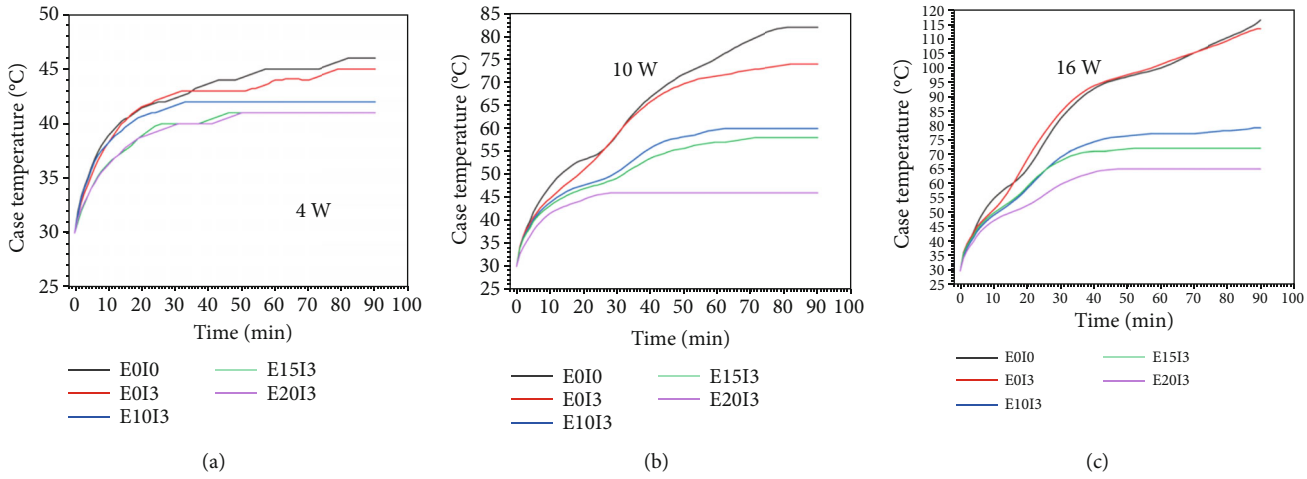

Figure 5: LED case temperature versus time for different configurations of heat sinks with PCM at various input powers: (a) 4 W, (b) 10 W, and (c) 16 W.

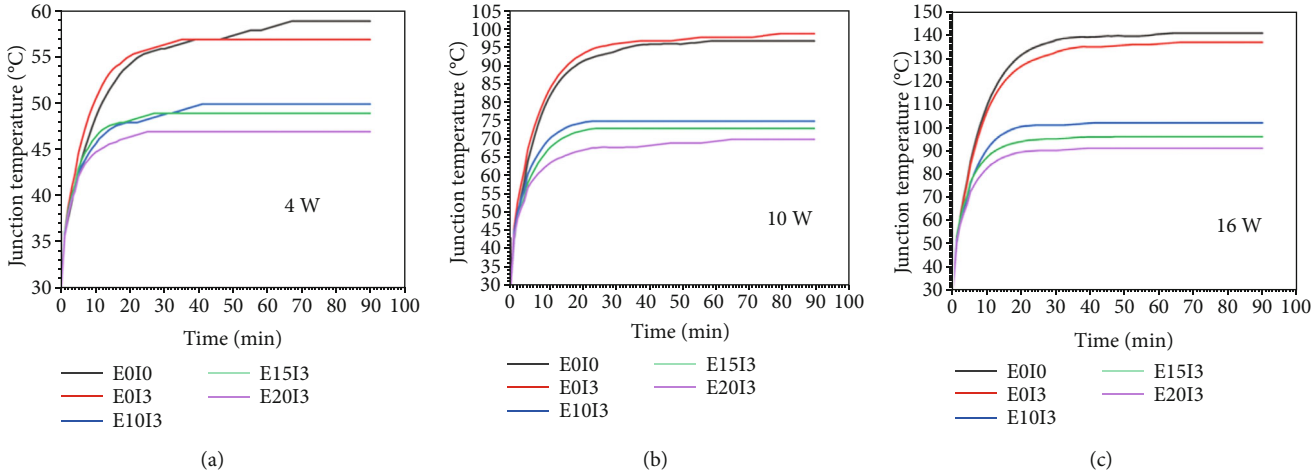

Figure 6: Junction temperatures versus time taken for various configurations of the heat sink without PCM at various input powers: (a) 4 W, (b) 10 W, and (c) 16 W.

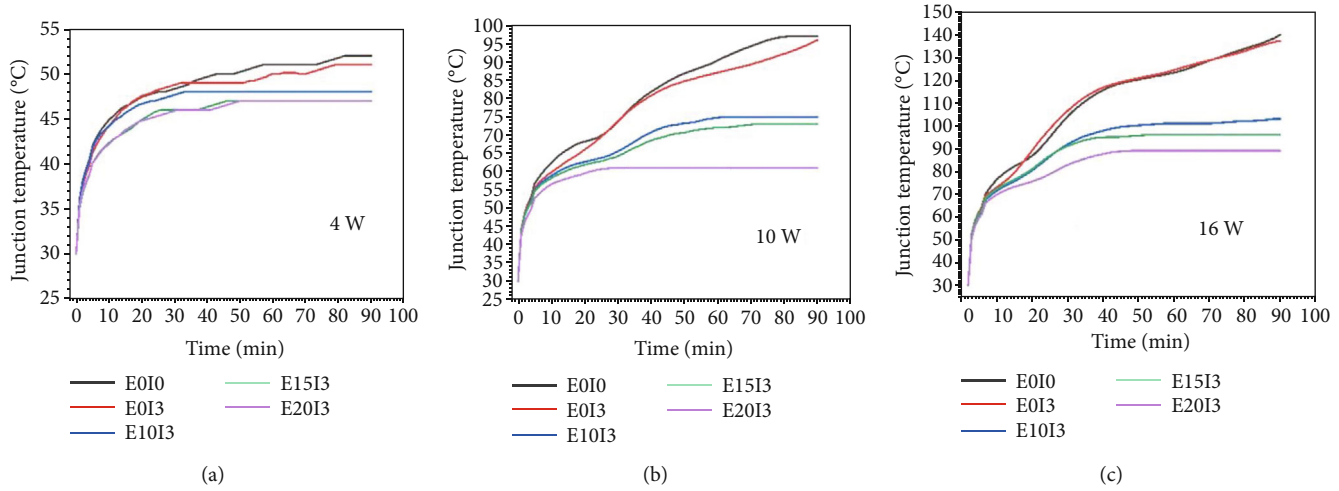

Figure 7: Junction temperature versus the time for different configurations of heat sinks containing PCM at various input powers: (a) 4 W, (b) 10 W, and (c) 16 W.

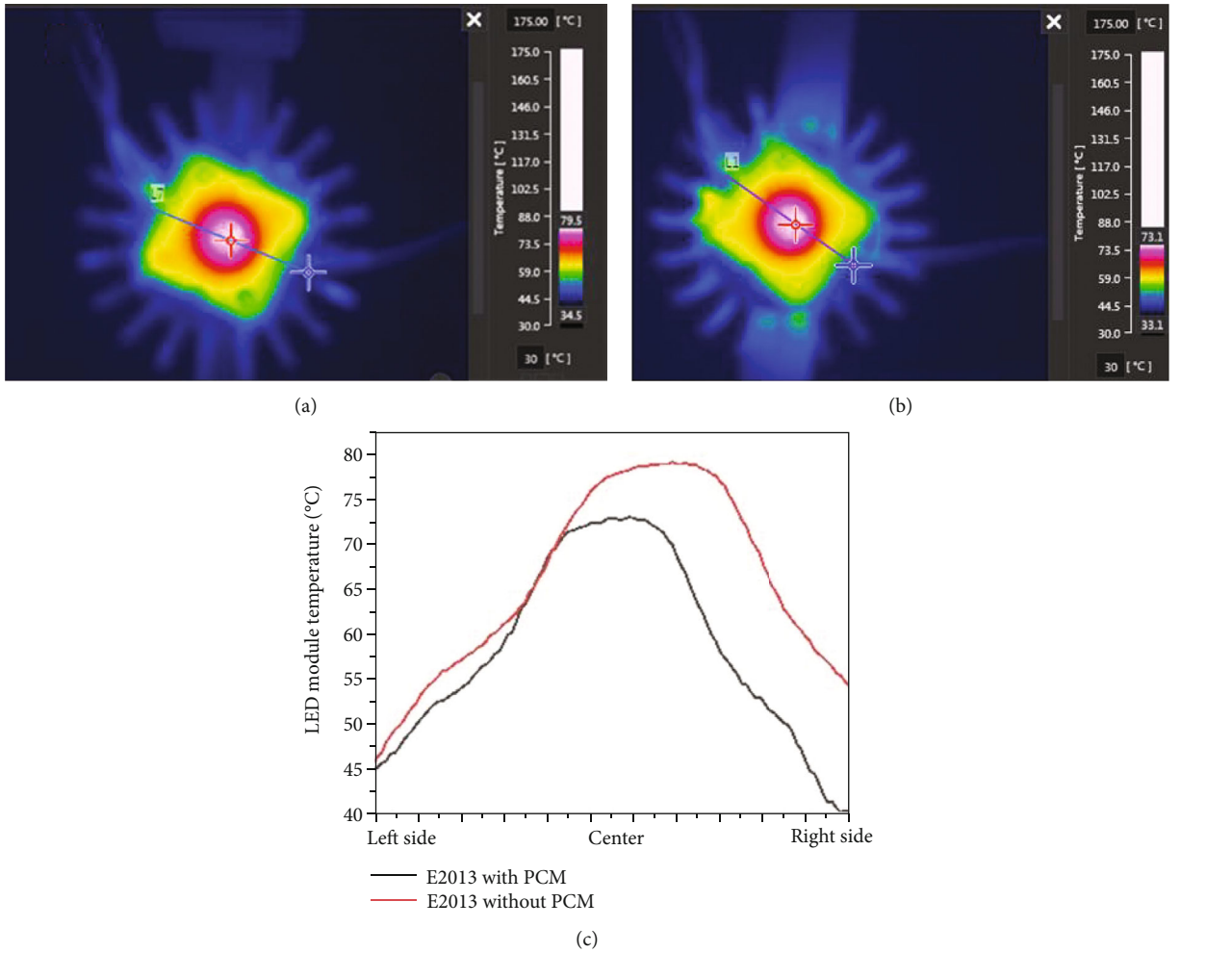

Figure 8: Temperature distribution of LED module (a) heat sink E20I3 without PCM and (b) heat sink E20I3 with PCM. (c) Temperature distribution along the lines in infrared thermal image camera.

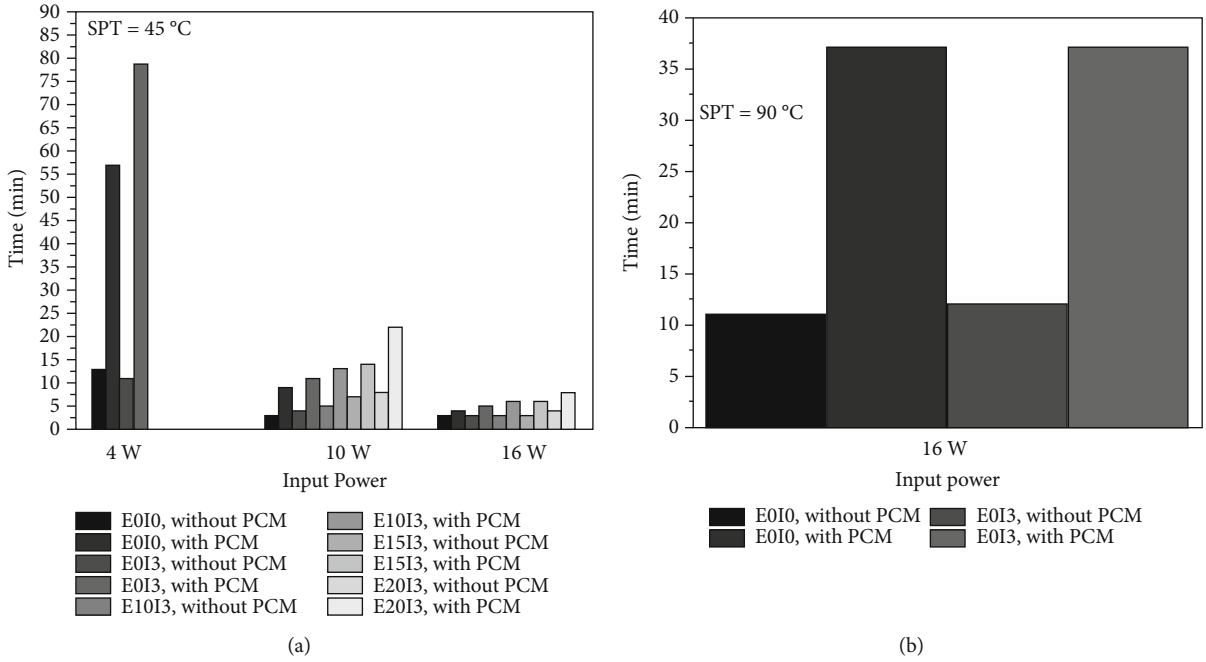

Figure 9: Critical time to reach SPTs. (a) 45°C and (b) 90°C.

E0I0, E0I3, E10I3, E15I3, and E20I3, respectively, at 4 W input power. Figure 6(b), when using heat sink E20I3 without PCM, significantly reduced the LED junction from 84°C to 55°C at 10 W, compared to the heat sink E0I0 without PCM. Also, for 16 W input power, the LED junction temperature is reduced. Therefore, it implies that by using the E20I3 sink, the LED can be operated at a lower temperature.

3.5. Junction Temperature Effect on Heat Sink Different Configuration (with PCM). The LED thermal management system relies heavily on the LED junction temperature because the LED's lifetime decreases as its temperature rises [39]. Figure 7(a) depicts the time-dependent LED junction temperature (Figure 7(c)). LED junction temperature dropped by 9°C, from a high of 70°C at 10 W to a low of 61°C when compared to heat sink E20I3 without and with PCM. At 16 W, it was also noted that the junction temperature of the LED dropped by 2°C, from 91°C to 89°C. In this case, the latent heat absorption of the PCM is primarily responsible for the lowered junction temperature. Because of this phenomenon, the heat transfer rate via convection through the exterior fins increased. The fins improve heat transfer and delay PCM melting by increasing convection. The delayed melting improves the LED junction's heat transfer.

3.6. Temperature Variation in LED Module. An infrared thermal image camera was utilized during this experimentation phase to record the LED unit's temperature variations. The LED module's temperature variation for the E20I3 heat sink filled and not filled with paraffin at 10 W is displayed in Figures 8(a)–8(c). The thermal images show that the LED modules in the paraffin-filled heat sink E20I3 were kept at a uniform and minimum temperature, while those in the heat sink E20I3 without PCM were kept at a temperature that was 6 degrees Celsius higher. This is because the junction temperature of the heat sink E20I3 without PCM was greater than that of the E20I3 with PCM. In Figure 6, we see the proof. In conclusion, the heat sink E20I3 equipped with PCM at 10 W input power can extend the life of the LEDs in the current investigation.

3.7. Enhancement of Operation Time of Various Heat Sink Configurations for Critical SPTs. This section estimates the positive effects of PCM-based heat sinks for high-power LED and also examined the duration during which LED case temperature is kept within the maximum temperature. The set point temperature (SPT) is the highest temperature at which high-power LEDs may operate without being damaged [13]. The essential SPT of 45°C and 90°C were used in this study. Figure 9 compares the duration at and below 45°C as well as 90°C for the paraffin filled and not filled with heat sinks at 4 W, 10 W, and 16 W. Figure 9(a) results reveal that it takes more time to reach 45°C for the E20I3 heat sink with PCM, compared to other heat sinks. For input power, 10 W results indicated that the E20I3 heat sink with no PCM reached 45°C in 8 minutes, whereas the SPT was reached in 22 minutes using the PCM-filled heat sink E20I3. This discloses that heat sink E20I3 with PCM has triggered a decrement of 14 min to attain an SPT of 45°C due to PCM's latent heat storage capability. Similarly, heat sink E0I3 with PCM has instigated a delay of 68 min to achieve SPT of 45°C at 4 W input power. But heat sinks E10I3, E15I3, and E20I3 did not attain 45°C for both cases with and without PCM. Figure 9(b) compares the SPT at 90°C for different heat sink configurations at 16 W input power. The LED case temperatures of the heat sinks with and without any PCM have not yet reached 90°C under

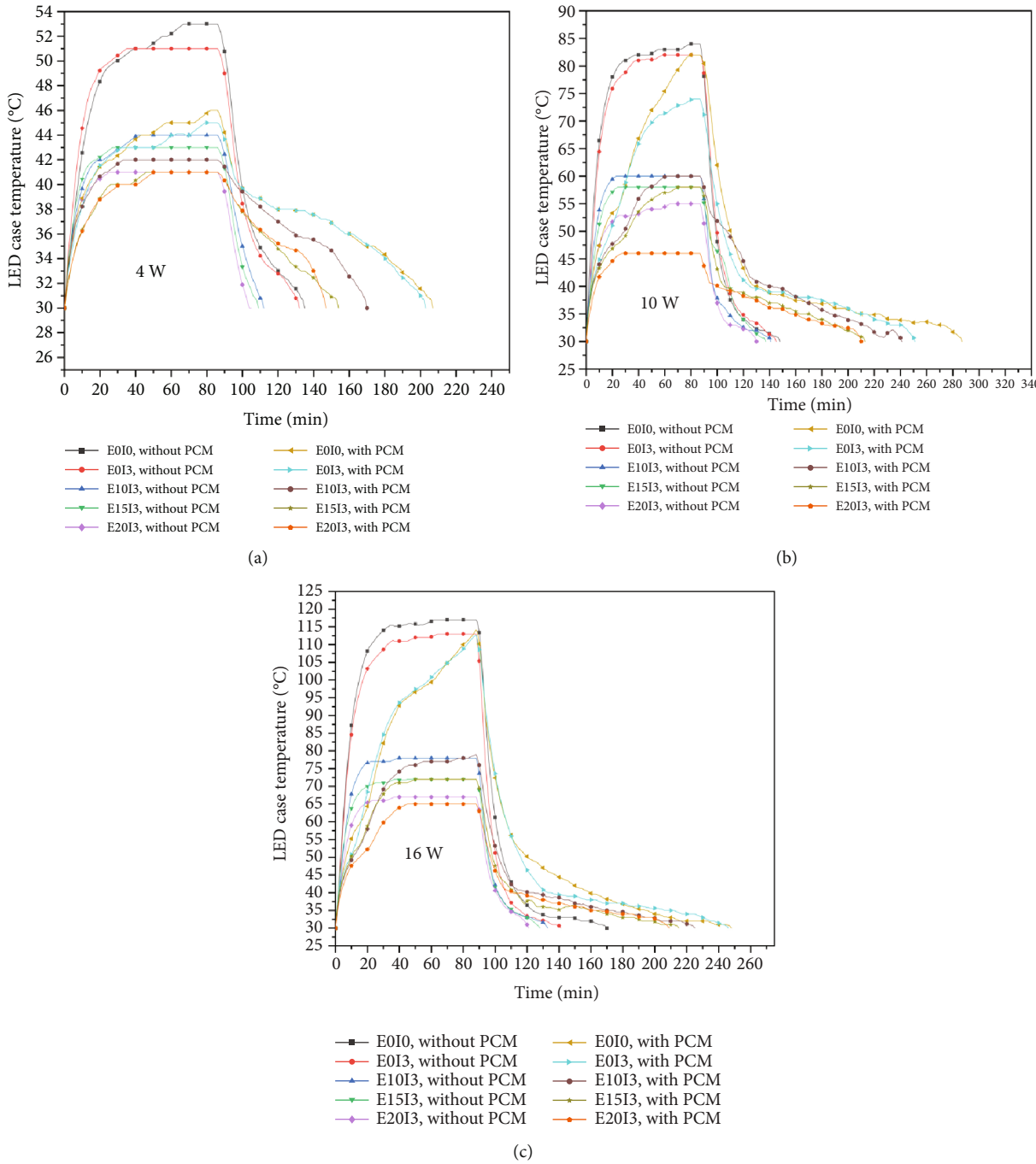

Figure 10: Heating and cooling rate of the heat sink that contains PCM and also its counterpart devoid of PCM. This shows LED case temperature variation with time.

4 W and 10 W. For 16 W input, there is no significant performance because of high-input power, using heat sink E20I3 with PCM to operate reliably for long-time use.

3.8. Effect of Different Heat Sink Configuration Heat Charging and Discharge Rate Analysis. The heat charging, as well as the rate of heat release of the heat sink with and without PCM, were analyzed using the time-varying LED heating and cooling experiments. The effectiveness of heat sink configuration on PCM's storage and dissipation ability was observed by comparing the paraffin filled and not filled with heat sinks at 4 W, 10 W, and 16 W input power. This is depicted in Figures 10(a)–10(c). The LED T_c difference for the heat E0I0, E0I3, E10I3, E15I3, and E20I3 with PCM took 17 min, 16 min, 16 min, 15 min, and 26 min to attain 65°C during the heating process at 16 W input power. The PCM melting rate is low with the help of more surface area heat sink contact with the surrounding. In case during the heat cooling process, heat sinks E0I0, E0I3, E10I3, E15I3, and E20I3 without

Table 4: Three modes of LED module operation condition.

Cyclic mode	Operation sequences of the LED module			
	Input power on (min)	Input power off (min)	Cycles	User condition
M-I	15	15	3	Light
M-II	30	30	3	Moderate
M-III	45	45	3	Heavy

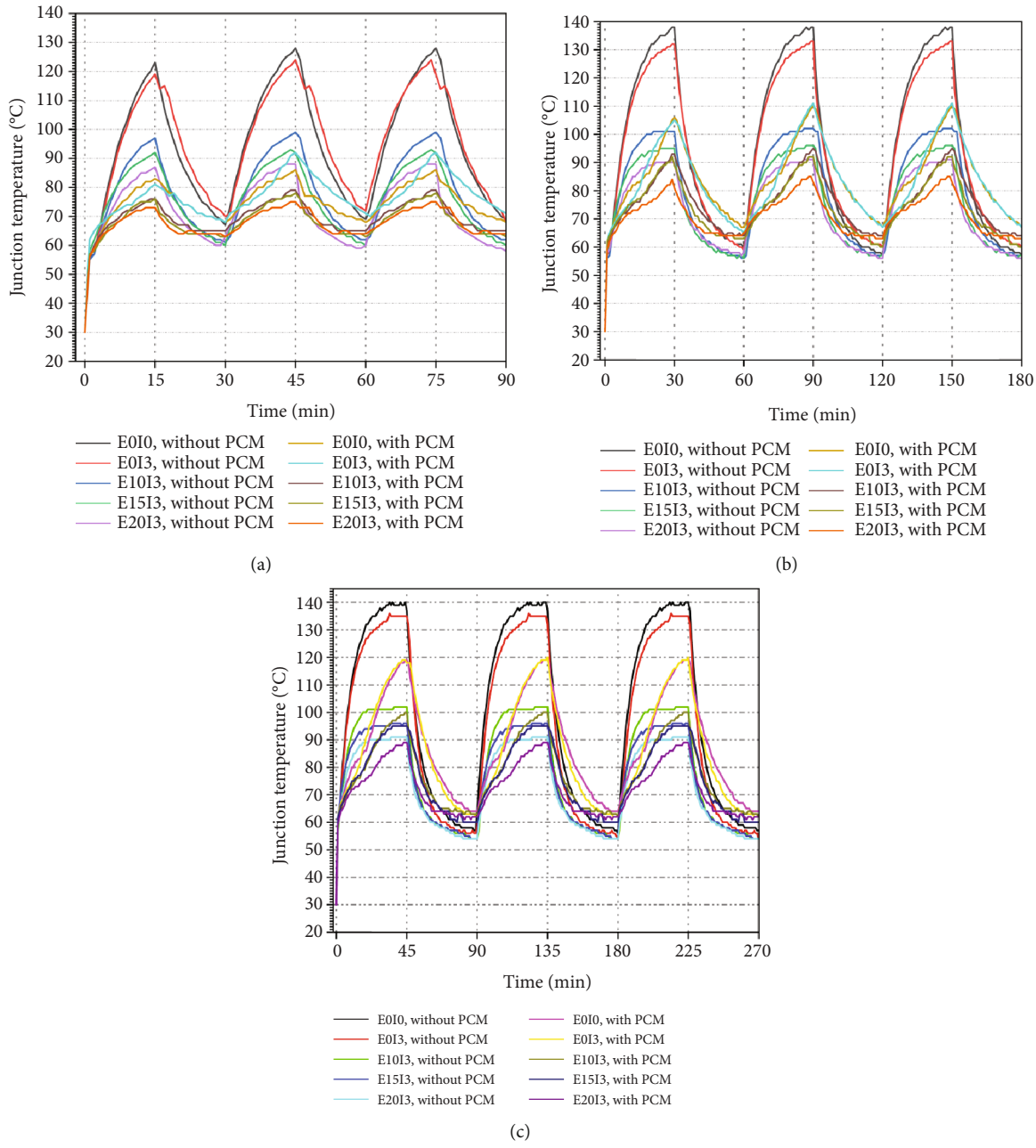

Figure 11: LED junction temperature changes of the heat sinks E0I0, E0I3, E10I3, E15I3, and E20I3 with and without PCM under (a) Mode-I, (b) Mode-II, and (c) Mode-III.

PCM are provided at LED case temperature that took 170 min, 141 min, 133 min, 128 min, and 121 min, respectively, to reach ambient temperature 30°C. But in the same heat sinks with PCM, LED case temperature took a long time to reach ambient temperature because of more heat stored in PCM-based sinks. Here, clearly recommend the heat E20I3 sink with PCM suitable for high-power LED thermal management system.

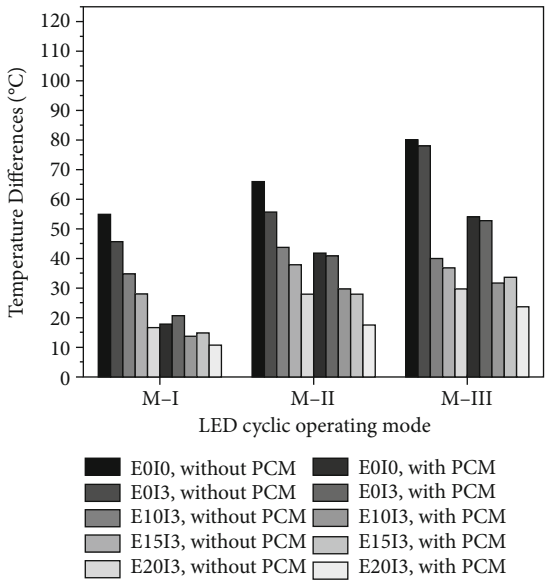

Figure 12: The temperature difference between the maximum and minimum temperature during the cyclic operation cycle of LED module heat sink with and without PCM under three different mode conditions.

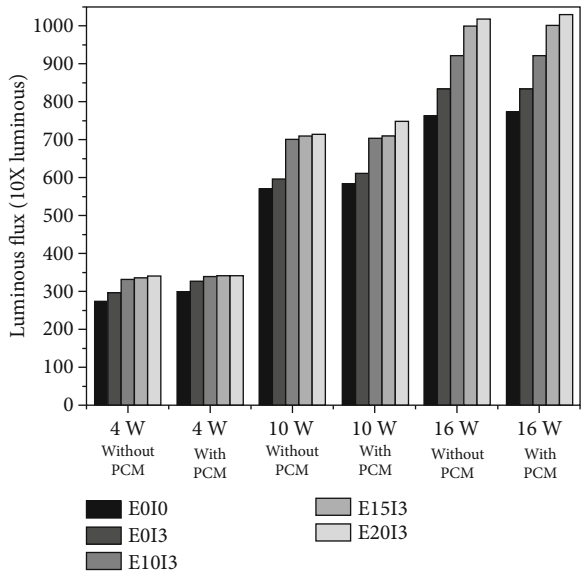

Figure 13: Performance of the luminous flux of the LED module operating at various input powers.

3.9. Different Configuration Heat Sink under Intermittent Load. LEDs are typically used daily in a variety of applications, with each one requiring a unique cycle of operation. Table 4 displays the results of an analysis done on the performance of the PCM-based heat sink used in the heat exchanger under three different cyclic operation modes (M-I, M-II, and M-III) at 16 W input power. As shown in Figure 11, the junction temperature tends to stabilize in all modes after the second working cycle. In the third working cycle (the last), the peak LED junction temperatures for Case M-1, light users, using heat sinks E0I0 and E20I3 without PCM are 124°C and 75°C, respectively, with a temperature fluctuation of 49°C. Figure 12 is a histogram

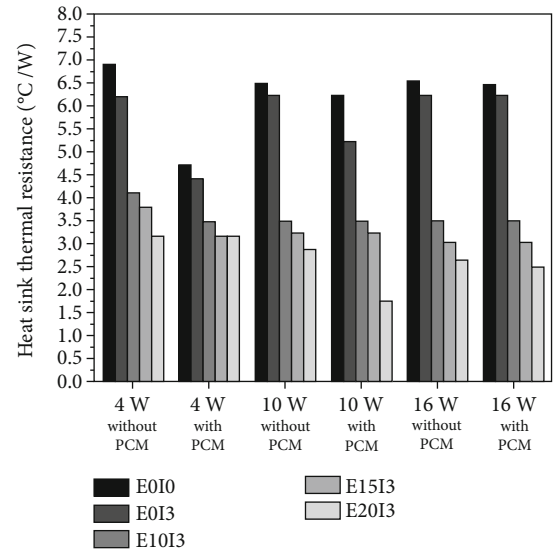

Figure 14: Effect of with and without PCM on heat sink thermal resistance for different input power.

representation of the temperature data taken from Figures 11(a)–11(c). In Figure 13, we see the LED module and heat sink's maximum and minimum temperatures across three mode conditions, with and without PCM. The second M-II mode is the middle-of-the-road operating setting. When comparing the E20I3 and E10I3 heat sinks with PCM, the LED junction's maximum and minimum temperatures are 81 degrees Celsius and 63 degrees Celsius, respectively, with temperature fluctuations of 18 degrees Celsius and 30 degrees Celsius, respectively. The third mode of operation represents the M-III heavy mode of operation. LED junction temperatures (i.e., maximum and minimum) are 86°C and 62°C versus 94°C and 62°C, respectively, with a temperature change of 24°C and 32°C when using a heat sink, E20I3, and E10I3 with PCM. The results show that the PCM completely decomposes during this mode, according to the findings. The results demonstrate that PCM in the heat sink enhanced the performance of the heat sink by smoothing the peat temperature curve in intermittent power operation mode.

3.10. Performance of Luminous Flux. The LED module's luminous flux at 4 W, 10 W, and 16 W is depicted in Figure 13. Using a lux meter, the LED module's luminous flux was measured once its junction temperature had stabilized. According to the numbers in Figure 13, the heat sink with the code E20I3 and no PCM has a luminous flux of 715 lm at 10 W. While the E20I3 without PCM has a 650 lm lumen output at the same input power, the PCM-containing version has a 750 lm lumen output, an increase of 4.7%. This component achieves significantly better performance thanks to a lower junction temperature compared to heat sink E20I3 without PCM.

3.11. Heat Sink Thermal Resistance. The thermal resistance of the heat sink is calculated at steady-state temperature conditions using equation (5) to investigate the heat transfer performance. Figure 14 shows the thermal resistance of

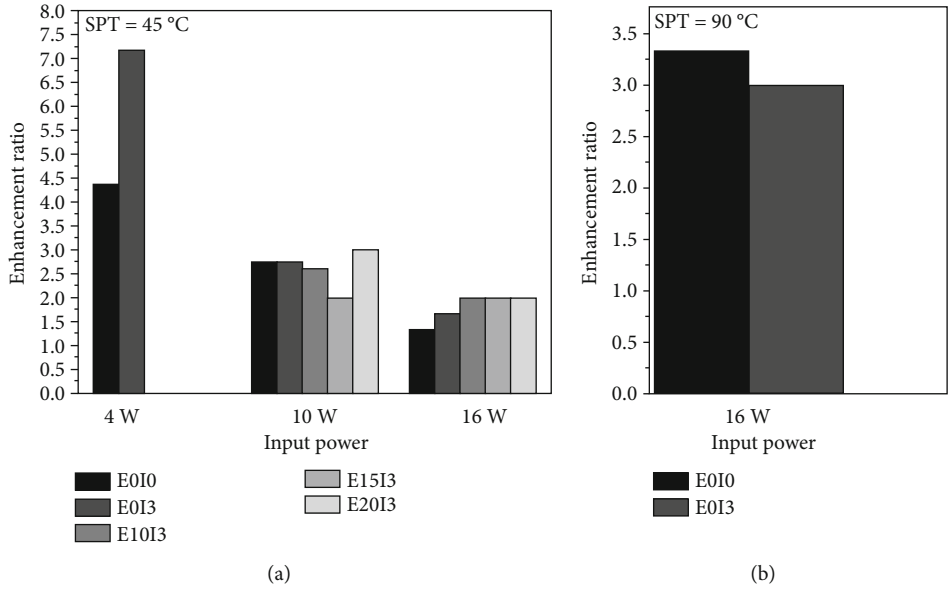

Figure 15: Enhancement ratio.

different configuration heat sinks E0I0, E0I3, E10I3, E15I3, and E20I3 with and without PCM. From Figure 14, the thermal resistances of the heat sink without PCM are higher than those of the heat sink with PCM at all input power. The thermal resistance of the heat sink E20I3 with PCM is 1.76°C/W, which is 38.19% lower than that of the heat sink E20I3 without PCM at 10 W input power. The first reason is that the PCM during the phase change process (i.e., solid to liquid) receives massive heat energy (i.e., latent heat). The second reason that the thermal resistance has decreased is due to the heat transfer mechanism of convection and conduction.

3.12. Enhancement Ratio for Various Configurations of the Heat Sinks with PCM. The improvement ratio is a quantitative value. For high-power LED thermal management, a PCM-filled heat sink is employed. This method is employed to determine how various heat sink configurations affect its heat dissipation rate. A paraffin-filled heat sink has a shorter time to reach its critical set point temperature than a heat exchanger without PCM, as defined by the enhancement ratio. Equation (6) was used to figure out the PCM enhancement ratio, depicted in Figure 15.

$$\epsilon_{\text{PCM}} = \frac{t_{\text{cr with PCM}}}{t_{\text{cr without PCM}}}. \tag{6}$$

Figure 15(a) depicts the temperature at which the SPT enhancement ratio reaches its maximum. Input power of 4 W causes the heat sinks E0I0 and E0I3 to reach an enhancement ratio of 4.3 and 7.1, respectively. From this, we can deduce that heat sink E0I3 has the highest enhancement ratio, indicating that the PCM underwent the phase change process, whereas heat sinks with the same input power as E0I3 fail to reach SPT of 45°C. E20I3 has a maximum enhancement ratio of 3 compared to other heat sinks when the power input is 10 W. Figure 15(b) demonstrates that the enhancement ratio obtained at 90°C is lower than that at lower temperatures due to the rapid increase in temperature in the region after complete melting. For high-input-power LED lighting applications, it is concluded that PCM with more radial-finned heat sinks is more efficient.

4. Conclusion

Investigating the heat transfer performance of the paraffin-filled heat sinks and then understanding the LED thermal enhancement, the paraffin-filled-based heat sinks are used. The findings are as follows:

(i) The heat dissipation performance of the paraffin not filled with heat sink E20I3 was better to reduce the T_j of a high-power LED module significantly, compared to other heat sinks without paraffin, and it can reduce the T_j up to 50°C, compared to the paraffin not filled with heat sink E0I0 at 16 W input power

(ii) The paraffin-filled-based heat sink results in a more impressive heat transfer performance. The LED T_j heat sink E20I3 with paraffin is 9°C lower than the heat sink E20I3 without paraffin at 10 W. Moreover, the heat sink E20I3 with paraffin extends the LED module's crucial lifetime

(iii) High-power LED lighting system is investigated using intermittent load conditions. It is observed that the peak temperature was reduced and, consequently, an extended operating of LEDs

(iv) Due to reducing the LED T_j and Rh, it increases the luminous flux. This shows that the luminous flux of the paraffin-not-filled heat sink E20I3 was 715 lm at 10 W. And that of the paraffin-filled heat sink E20I3

was 750 lm at the same input power, and it is about 4.7% higher than that of the E20I3 without paraffin

(v) For input power, 10 W results in an exhibit that the E20I3 heat sink did not have any phase change material at 45°C within 8 min, whereas the same SPT was attained using heat sink E20I3 with PCM in 22 min. This shows that the purpose of heat sink E20I3 with phase change material has enabled a delay of 14 min to obtain an SPT of 45°C due to PCM's latent heat storage capacity

(vi) An enhancement ratio of 4.3 and 7.1 is obtained for the heat sinks E0I0 and E0I3, respectively, at 4 W input power

Data Availability

All data that support the findings of this study are included within this article.

Conflicts of Interest

The authors declare that they have no conflicts of interest.

Acknowledgments

The authors extend their appreciation to King Saud University for funding this work through the Researchers Supporting Project number (RSPD2023R711), King Saud University, Riyadh, Saudi Arabia.

References

[1] Y. Tang, Q. Chen, W. Guan, Z. Li, B. Yu, and W. Yuan, "Thermal analysis of an LED module with a novelly assembled heat pipe heat sink," *Journal of Central South University*, vol. 24, no. 4, pp. 921–928, 2017.

[2] H. Wang, J. Qu, Y. Peng, and Q. Sun, "Heat transfer performance of a novel tubular oscillating heat pipe with sintered copper particles inside flat-plate evaporator and high-power LED heat sink application," *Energy Conversion and Management*, vol. 189, pp. 215–222, 2019.

[3] N. Narendran and Y. Gu, "Life of LED-based white light sources," *Journal of Display Technology*, vol. 1, no. 1, pp. 167–171, 2005.

[4] X. Lin, S. Mo, B. Mo, L. Jia, Y. Chen, and Z. Cheng, "Thermal management of high-power LED based on thermoelectric cooler and nanofluid-cooled microchannel heat sink," *Applied Thermal Engineering*, vol. 172, article 115165, 2020.

[5] M. W. Jeong, S. W. Jeon, and Y. Kim, "Optimal thermal design of a horizontal fin heat sink with a modified-opening model mounted on an LED module," *Applied Thermal Engineering*, vol. 91, pp. 105–115, 2015.

[6] C. Huang and G. Wang, "A design problem to estimate the optimal fin shape of LED lighting heat sinks," *International Journal of Heat and Mass Transfer*, vol. 106, pp. 1205–1217, 2016.

[7] D. S. Huang, T. C. Chen, L. Te Tsai, and M. T. Lin, "Design of fins with a grooved heat pipe for dissipation of heat from high-powered automotive LED headlights," *Energy Conversion and Management*, vol. 180, pp. 550–558, 2018.

[8] S. Park, D. Jang, S. Yook, and K. Lee, "Optimization of a chimney design for cooling efficiency of a radial heat sink in a LED downlight," *Energy Conversion and Management*, vol. 114, pp. 180–187, 2016.

[9] S. Sundar, G. Song, M. Z. Zahir, J. S. Jayakumar, and S. J. Yook, "Performance investigation of radial heat sink with circular base and perforated staggered fins," *International Journal of Heat and Mass Transfer*, vol. 143, article 118526, 2019.

[10] S. Yu, K. Lee, and S. Yook, "Natural convection around a radial heat sink," *International Journal of Heat and Mass Transfer*, vol. 53, no. 13–14, pp. 2935–2938, 2010.

[11] S. S. Haghighi, H. R. Goshayeshi, and M. R. Safaei, "Natural convection heat transfer enhancement in new designs of plate-fin based heat sinks," *International Journal of Heat and Mass Transfer*, vol. 125, pp. 640–647, 2018.

[12] S. Feng, M. Shi, H. Yan, S. Sun, F. Li, and J. Lu, "Natural convection in a cross-fin heat sink," *Applied Thermal Engineering*, vol. 132, pp. 30–37, 2018.

[13] Y. Wu, Y. Tang, Z. Li et al., "Experimental investigation of a PCM-HP heat sink on its thermal performance and anti-thermal-shock capacity for high-power LEDs," *Applied Thermal Engineering*, vol. 108, pp. 192–203, 2016.

[14] J. Zmywaczyk, P. Zbińkowski, H. Smogór, A. Olejnik, and P. Koniorczyk, "Cooling of high-power LED lamp using a commercial paraffin wax," *International Journal of Thermophysics*, vol. 38, no. 3, pp. 1–14, 2017.

[15] T. Ramesh, A. S. Praveen, P. B. Pillai, and S. Salunkhe, "Phase change material aided thermal scheming of high power LED: effect of PCM with varying pitch of hexagonal fins," *Materials Research Innovations*, vol. 25, no. 7, pp. 1–10, 2021.

[16] T. Ramesh, A. S. Praveen, P. B. Pillai, and S. Salunkhe, "Numerical simulation of heat sinks with different configurations for high power LED thermal management," *International Journal for Simulation and Multidisciplinary Design Optimization*, vol. 13, p. 18, 2022.

[17] T. Ramesh, A. S. Praveen, and P. B. Pillai, "Experimental investigation of carbon nanotube coated heat sink for LED thermal management," *Materials Today: Proceedings*, vol. 68, pp. 2099–2103, 2022.

[18] S. K. Sahoo, M. K. Das, and P. Rath, *Application of TCE-PCM based heat sinks for cooling of electronic components: a review, vol. 59*, Elsevier, 2016.

[19] R. Baby, C. Balaji, and H. Transfer, *Experimental heat transfer: a journal of thermal energy generation, transport, storage, and conversion a neural network-based optimization of thermal performance of phase change material-based finned heat sinks – an experimental study*, Elsevier, 2015.

[20] A. Sharma, V. V. Tyagi, C. R. Chen, and D. Buddhi, "Review on thermal energy storage with phase change materials and applications," *Renewable and Sustainable Energy Reviews*, vol. 13, no. 2, pp. 318–345, 2009.

[21] E. M. S. El-Said, G. B. Abdelaziz, S. W. Sharshir, A. H. Elsheikh, and A. M. Elsaid, "Experimental investigation of the twist angle effects on thermo-hydraulic performance of a square and hexagonal pin fin array in forced convection," *International Communications in Heat and Mass Transfer*, vol. 126, article 105374, 2021.

[22] M. Ahmadein, A. H. Elsheikh, and N. A. Alsaleh, "Modeling of cooling and heat conduction in permanent mold casting process," *Alexandria Engineering Journal*, vol. 61, no. 2, pp. 1757–1768, 2022.

[23] K. K. Ghosh, C. R. Sonawane, A. Pandey et al., "Experimental investigations on indirect contact type liquid desiccant cooling systems for high latent heat load application," *Case Studies in Thermal Engineering*, vol. 31, article 101814, 2022.

[24] A. H. Elsheikh, J. Guo, Y. Huang, J. Ji, and K.-M. Lee, "Temperature field sensing of a thin-wall component during machining: numerical and experimental investigations," *International Journal of Heat and Mass Transfer*, vol. 126, pp. 935–945, 2018.

[25] A. H. Elsheikh, J. Guo, and K.-M. Lee, "Thermal deflection and thermal stresses in a thin circular plate under an axisymmetric heat source," *Journal of Thermal Stresses*, vol. 42, no. 3, pp. 361–373, 2019.

[26] M. J. Ashraf, H. M. Ali, H. Usman, and A. Arshad, "Experimental passive electronics cooling: parametric investigation of pin-fin geometries and efficient phase change materials," *International Journal of Heat and Mass Transfer*, vol. 115, pp. 251–263, 2017.

[27] E. M. S. El-Said, M. A. Elaziz, and A. H. Elsheikh, "Machine learning algorithms for improving the prediction of air injection effect on the thermohydraulic performance of shell and tube heat exchanger," *Applied Thermal Engineering*, vol. 185, article 116471, 2021.

[28] S. F. Hosseinizadeh, F. L. Tan, and S. M. Moosania, "Experimental and numerical studies on performance of PCM-based heat sink with different configurations of internal fins," *Applied Thermal Engineering*, vol. 31, no. 17–18, pp. 3827–3838, 2011.

[29] Z. Li, Y. Wu, B. Zhuang et al., "Preparation of novel copper-powder-sintered frame/paraffin form-stable phase change materials with extremely high thermal conductivity," *Applied Energy*, vol. 206, pp. 1147–1157, 2017.

[30] O. K. Yagci, M. Avci, and O. Aydin, "Melting and solidification of PCM in a tube-in-shell unit: Effect of fin edge lengths' ratio," *Journal of Energy Storage*, vol. 24, article 100802, 2019.

[31] A. Arshad, H. M. Ali, M. Ali, and S. Manzoor, "Thermal performance of phase change material (PCM) based pin-finned heat sinks for electronics devices: effect of pin thickness and PCM volume fraction," *Applied Thermal Engineering*, vol. 112, pp. 143–155, 2017.

[32] B. Praveen and S. Suresh, "Thermal performance of micro-encapsulated PCM with LMA thermal percolation in TES based heat sink application," *Energy Conversion and Management*, vol. 185, pp. 75–86, 2019.

[33] B. Praveen, S. Suresh, and V. Pethurajan, "Heat transfer performance of graphene nano-platelets laden micro-encapsulated PCM with polymer shell for thermal energy storage based heat sink," *Applied Thermal Engineering*, vol. 156, pp. 237–249, 2019.

[34] B. Praveen and S. Suresh, "Experimental study on heat transfer performance of neopentyl glycol/CuO composite solid-solid PCM in TES based heat sink," *Engineering Science and Technology, an International Journal*, vol. 21, no. 5, pp. 1086–1094, 2018.

[35] K. P. Venkitaraj, S. Suresh, B. Praveen, and S. C. Nair, "Experimental heat transfer analysis of macro packed neopentylglycol with CuO nano additives for building cooling applications," *Journal of Energy Storage*, vol. 17, pp. 1–10, 2018.

[36] K. P. Venkitaraj, S. Suresh, and B. Praveen, "Experimental charging and discharging performance of alumina enhanced pentaerythritol using a shell and tube TES system," *Sustainable Cities and Society*, vol. 51, article 101767, 2019.

[37] R. Baby and C. Balaji, "Thermal optimization of PCM based pin fin heat sinks: an experimental study," *Applied Thermal Engineering*, vol. 54, no. 1, pp. 65–77, 2013.

[38] Z. Deng, C. Zhang, Q. Sun, L. Wu, F. Yao, and D. Xu, "Experimental study on melting performance of phase change material - based finned heat sinks by a comprehensive evaluation," *Journal of Thermal Analysis and Calorimetry*, vol. 144, article 123456789, pp. 869–882, 2020.

[39] A. Rammohan and V. P. Chandramohan, "Experimental analysis on estimating junction temperature and service life of high power LED array," *Microelectronics Reliability*, vol. 120, article 114121, 2021.